arXiv:1204.6682v2 [cond-mat.str-el] 2 Aug 2012

Simplex solids in SU(N) Heisenberg models on the kagome and checkerboard lattices

Philippe Corboz,[1] Karlo Penc,[2,3] Frédéric Mila,[4] and Andreas M. Läuchli[5,6]

[1]*Theoretische Physik, ETH Zürich, CH-8093 Zürich, Switzerland*
[2]*Institute for Solid State Physics and Optics, Wigner Research Centre for Physics, Hungarian Academy of Sciences, H-1525 Budapest, P.O.B. 49, Hungary*
[3]*Department of Physics, Budapest University of Technology and Economics and Condensed Matter Research Group of the Hungarian Academy of Sciences, 1111 Budapest, Hungary*
[4]*Institut de théorie des phénomènes physiques, École Polytechnique Fédérale de Lausanne, CH-1015 Lausanne, Switzerland*
[5]*Institut für Theoretische Physik, Universität Innsbruck, A-6020 Innsbruck, Austria*
[6]*Max-Planck-Institut für Physik komplexer Systeme, Nöthnitzer Straße 38, D-01187 Dresden, Germany*

(Dated: March 3, 2013)

We present a numerical study of the SU(N) Heisenberg model with the fundamental representation at each site for the kagome lattice (for $N = 3$) and the checkerboard lattice (for $N = 4$), which are the line graphs of the honeycomb and square lattices and thus belong to the class of bisimplex lattices. Using infinite projected entangled-pair states (iPEPS) and exact diagonalizations, we show that in both cases the ground state is a simplex solid state with a two-fold degeneracy, in which the N spins belonging to a simplex (*i.e.* a complete graph) form a singlet. Theses states can be seen as generalizations of valence bond solid states known to be stabilized in certain SU(2) spin models.

PACS numbers: 67.85.-d, 71.10.Fd, 75.10.Jm, 02.70.-c

I. INTRODUCTION

The SU(2) Heisenberg model on the square lattice is one of the most studied systems in condensed matter physics, and its properties are by now well understood. Generalizations of this model to SU(N) with different values of N, lattice geometries, and representations of SU(N) exhibit an extremely rich variety of different ground states. While such models have been the subject of many theoretical studies in the past decades,[1–9] they have recently attracted increasing interest thanks to the proposals to realize SU(N) symmetric Hubbard models in experiments on ultracold fermionic atoms in optical lattices.[10–13]

As in the SU(2) case, the SU(N) Heisenberg models can be derived from a generalized Hubbard model of N flavors of fermions in a Mott insulating phase. Different numbers of particles per site correspond to different representations of SU(N). In this work we focus on the Heisenberg model with one particle per site, corresponding to the fundamental representation (a Young diagram with a single box) of SU(N) at each site. The Hamiltonian can be written in terms of a permutation operator P_{ij}[14] which exchanges the particles on neighboring sites,

$$\mathcal{H} = \sum_{\langle i,j \rangle} P_{ij}. \tag{1}$$

The expectation value of the operator P_{ij} is minimal (and equal to -1) when the wave function is antisymmetric on the ij bond. For SU(N), a fully antisymmetric wave function can be constructed using exactly N sites (and not only two sites as in the familiar SU(2) case). This is an SU(N) singlet, and the energy on any bond belonging to the singlet reaches its lowest possible value -1. This should be contrasted to the other class of SU(N) Heisenberg models,[2–7] where conjugate representations on two different sublattices were used, and thus singlets can be formed between two sites for any N.

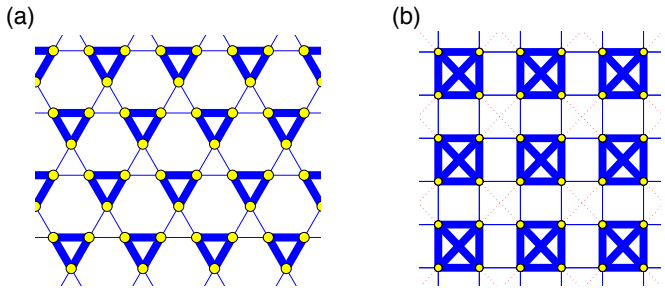

FIG. 1: (Color online) The simplex solid states obtained with iPEPS ($D = 14$) for two different SU(N) Heisenberg models. The width of a bond is proportional to the magnitude of the bond energy, while blue (red dotted) bonds correspond to negative (positive) energies. (a) One of the two degenerate trimerized ground states of the SU(3) Heisenberg model on the kagome lattice. (b) One of the two quadrumerized ground states of the SU(4) Heisenberg model on the checkerboard lattice.

In this work we study the model on a particular class of lattices, so-called bisimplex lattices,[15] consisting of corner sharing simplices residing on an underlying bipartite lattice (equivalent to the line graph of the underlying bipartite lattice). In particular, we investigate the possibility of having an N-merized ground state, i.e. where the lattice is covered by singlets which extend over N-site simplices.[48] Such *simplex solid states*[49] can be seen as a generalization of the valence bond solids (or valence bond crystals) known from certain SU(2) models, as for example the dimerized state in the Majumdar-Gosh model. Examples we consider here are the kagome lattice with 3-site simplices (triangles), and the checkerboard lattice with 4-site simplices (crossed-squares in Fig. 1(b), which are topologically equivalent to tetrahedra). Because of the underlying bipartite lattice (honeycomb for kagome, square for checkerboard) there are two possible ways

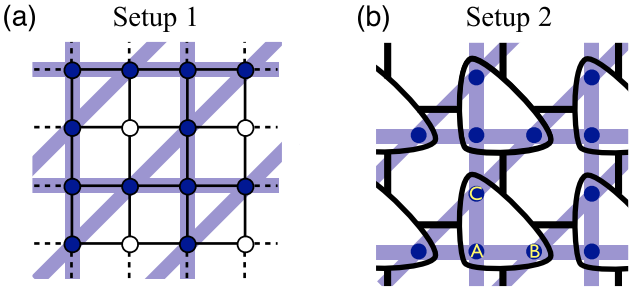

FIG. 2: (Color online) The two different simulation setups used to simulate the kagome lattice with the iPEPS method developed for the square lattice. Black circles and triangles correspond to tensors, black lines to connection between tensors (the physical index of a tensor is not shown). Interactions between physical sites (filled circles) are given by thick shaded lines. (a) Auxiliary tensors (white circles) are introduced to create a square lattice iPEPS. The interactions along the horizontal and vertical direction correspond to nearest-neighbor couplings on the square lattice, whereas the interactions along the diagonal are treated as next-nearest neighbor interactions. (b) Three physical sites A, B, C on the kagome lattice, each having a local dimension $d = 3$, are mapped into a block site with a local dimension $\tilde{d} = 27$.

to cover the lattice with singlets leading to a two-fold ground state degeneracy.

The occurrence of a symmetry broken state with a two-fold degeneracy on these lattices has already been observed in Refs. 16,17 for a t-J model away from half filling, which showed that this type of symmetry breaking is a likely candidate on these lattices. In Ref. 18 Arovas derived parent Hamiltonians for the exact SU(N) simplex solid states on the kagome (for $N = 3$) and the checkerboard lattice (for $N = 4$). It is conceivable that these parent Hamiltonians are adiabatically connected to the SU(N) Heisenberg model, in the same way as the Affleck-Kennedy-Lieb-Tasaki (AKLT) state[19] is adiabatically connected with the ground state of the $S = 1$ spin chain. Simplex solid states on bisimplex lattices have also been predicted in Ref. 9 based on studies of a particular large N limit, with representations labelled by Young tableaus with m rows and n_c columns, where $N/m = k$ and n_c are held fixed.

We use infinite projected entangled-pair states (iPEPS) and exact diagonalization (ED) to study the ground state of the $N = 3$ case on the kagome and the $N = 4$ case on the checkerboard lattice. Both methods consistently predict a two-fold degenerate simplex solid ground state for both models, summarized in Fig. 1.

The paper is organized as follows: In Sec. II we provide details on the iPEPS simulations, in particular, how the models are simulated using a square-lattice iPEPS. In Secs. III and IV we present the iPEPS and ED results obtained for the kagome and the checkerboard model, respectively. Finally, Sec. V summarizes our findings.

II. INFINITE PROJECTED ENTANGLED-PAIR STATES (IPEPS)

A projected-entangled pair state (PEPS) is an efficient variational ansatz for two-dimensional ground state wave functions.[20–24] It can be seen as a natural extension of a matrix product state (MPS), the underlying ansatz of the famous density matrix renormalization group (DMRG) method.[25] The main idea is to represent a wave function by a trace of a product of tensors, with one tensor per lattice site. On the square lattice each tensor T^p_{ijkl} has five indices: one index p which carries the local Hilbert space of a lattice site with dimension d, and four indices i, j, k, l - the auxiliary bonds with bond dimension D - which connect to the four nearest-neighbor tensors. Thus, each tensor contains dD^4 variational parameters, and by varying D the accuracy of the ansatz can be systematically controlled. A bond dimension $D = 1$ simply corresponds to a product state (a site-factorized wave function), and upon increasing D quantum fluctuations (entanglement) can be taken into account in a systematic way.

Details on the iPEPS method for the square lattice can be found in Refs. 26–28, in particular how to *optimize* the tensors (i.e. finding the best variational parameters) and how to compute expectation values by *contracting* the tensor network (i.e. computing the trace of the product of all tensors). We performed similar iPEPS simulations already for the SU(4) Heisenberg model[29] and the triangular- and square-lattice SU(3) Heisenberg model.[30]

For the experts, we note that the optimization is done through an imaginary time evolution using the simple update,[27,31–33] and we have verified some simulation results also with the full update.[27] The corner-transfer matrix method[27,34,35] is used to contract the tensor network, where the error of the approximate contraction can be controlled by the boundary dimension χ. The simulation results in this work are extrapolated in χ, where the extrapolation error is small compared to the symbol sizes. To improve the efficiency of the simulations we used tensors with $\mathbb{Z}_q$ symmetry.[36,37]

To simulate the checkerboard model we use the usual square lattice iPEPS ansatz where we treat the diagonal couplings as next-nearest neighbor interactions as described in Ref. 38.

For the kagome lattice we implemented two different simulation setups based on a square lattice iPEPS, which have the advantage that existing algorithms for the optimization and contraction can be reused. For the first variant we use one tensor per lattice site, plus additional auxiliary tensors which are inserted to form a square lattice iPEPS, as sketched in Fig. 2(a). [The bond dimension of the auxiliary tensors can be chosen as $D = 1$ since all correlations are carried by the tensors on the physical sites.] The couplings along the horizontal and vertical direction correspond to nearest-neighbor couplings between two tensors, whereas the remaining bonds necessary to form the kagome lattice are represented by the next-nearest-neighbor bonds in the square lattice, which can be treated as explained in Ref. 38. In the second setup we map the kagome lattice onto a square lattice by blocking three sites as illustrated in Fig. 2(b). The original Hamiltonian is mapped

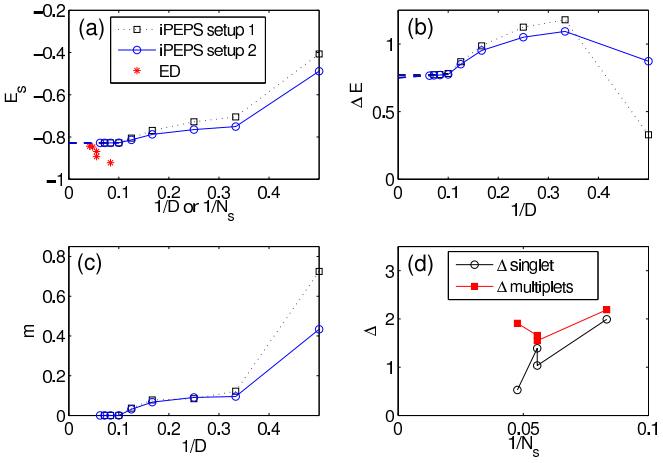

FIG. 3: (Color online) (a-c) iPEPS simulation results for the SU(3) Heisenberg model on the kagome lattice as a function of inverse bond dimension $1/D$ for the two simulation setups (cf. Fig. 2). Extrapolations (dashed lines) are a guide to the eye. (a) Energy per site compared with the results from ED (plotted as a function of $1/N_s$). The estimated value in the infinite D limit is $-0.829(1)$. (b) The difference in bond energies ΔE remains finite in the infinite D limit, which shows that the state breaks translational invariance as illustrated in Fig. 1(a). (c) Local moment which is strongly suppressed with increasing bond dimension. (d) ED results for the energy gaps to the first singlet and the first SU(3) multiplet excitations plotted as a function of the inverse number of sites $1/N_s$.

onto a square lattice Hamiltonian with nearest-neighbor interactions between the block sites (see supplementary material). We point out here that we do not block three sites belonging to a triangle in the kagome lattice, since this would automatically bias the solution towards a trimerized state.

Since we work directly in the thermodynamic limit, the ground state wave function may exhibit spontaneously broken symmetries. We measure the energy on each bond, E_b, in the unit cell. If the energies are not equal on all symmetry related bonds, i.e. if the difference

$$\Delta E = \max(E_b) - \min(E_b) \tag{2}$$

is finite, then the state breaks some lattice symmetries.

Furthermore, we compute the local ordered moment m on each site,

$$m = \sqrt{\frac{N}{N-1}\sum_{\alpha,\beta}\left(\langle S^\beta_\alpha\rangle - \frac{\delta_{\alpha\beta}}{N}\right)^2}, \tag{3}$$

where $S^\beta_\alpha = |\alpha\rangle\langle\beta|$ are the generators of SU(N) and α,β run over all flavor indices. A finite m implies that the SU(N) symmetry is broken.

We tried different unit cell sizes up to size 6×6 in iPEPS to test for possible stable color-ordered solutions, however all simulations consistently lead to an N-merized ground state. The results presented in the following are obtained with a 2×2 unit cell of tensors.

III. THE SU(3) MODEL ON THE KAGOME LATTICE

We consider the model (1) on the kagome lattice for $N = 3$ with the fundamental representation at each lattice site. Singlet formation most naturally occurs between three sites on a triangle, resulting into two possible coverings on the kagome lattice in which either all triangles pointing upwards, or all triangles pointing downwards form singlets. The latter case is illustrated in Fig. 1(a).

Figure 3(a) shows the iPEPS energy per site, E_s obtained with the two different simulation setups (cf. Fig. 2) as a function of bond dimension D. It is in general not known how quantities depend on D. Here we find that for $D > 10$ the energy does not change much anymore upon further increasing D. As an estimate in the infinite D limit we take the middle between the value at the maximal D and the value obtained from a linear extrapolation in $1/D$ for the four largest D.

From Fig. 3(b), it is clear that the difference between the highest and lowest bond energy ΔE is finite for all values of D, which indicates that the ground state breaks translational symmetry. The strength of the individual bond energies in the lattice can be seen in Fig. 1(a), where the thickness of a bond is proportional to the magnitude of the bond energy. The resulting pattern is clearly compatible with a trimerized state. The strength of the trimerization decreases with increasing D (except for the lowest $D = 2$), but it seems to remain finite around $\Delta E = 0.76(1)$ in the infinite D limit.

Since the trimerized state does not break the SU(3) symmetry, the local ordered moment m defined in Eq. (3) should vanish. Figure 3(c) shows that m is strongly suppressed with increasing D. In both simulation setups m vanishes completely for $D \geq 10$.

We note that we have also tested a 6×6 unit cell which can accommodate the $\sqrt{3}\times\sqrt{3}$ color ordered state predicted by linear flavor-wave theory (see Sec. V). We found that this state only appears as a metastable state in iPEPS, i.e., the N-merized ground state has a lower variational energy.

To further corroborate the iPEPS results we have performed ED simulations of the SU(3) Heisenberg model on finite size kagome samples of up to $N_s = 24$ sites (c.f. Ref. 39 regarding the geometry of the clusters). The energies per site have been included in Fig. 3(a) and the agreement between the two methods at large D or N_s is very good. In Fig. 3(d) we display two relevant energy gaps, the first one to the lowest singlet excitation at the Γ point, and the second one to the first magnetic (i.e. non-singlet) excitation. While the singlet gap seems to collapse for larger N_s, in agreement with the lattice symmetry breaking scenario requiring a two-fold ground state degeneracy, the magnetic gap appears to stay finite, in agreement with the picture of a nonmagnetic singlet ground state. In the left panel of Fig. 4 we finally show the connected bond energy correlations (cf. caption), which convincingly demonstrate the trimerization of the kagome lattice SU(3) Heisenberg model.

In summary, both iPEPS and ED provide strong indications that the ground state of the SU(3) Heisenberg model on the kagome lattice is trimerized.

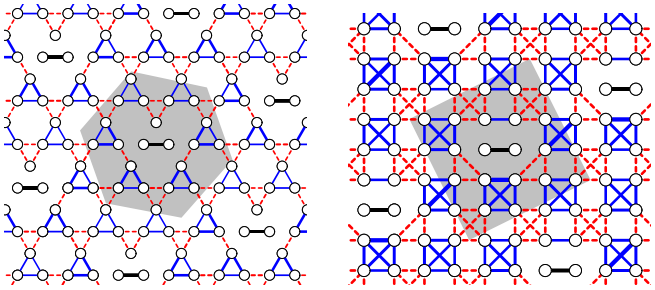

FIG. 4: (Color online) ED results for the connected bond energy correlations $\langle P_{ij}P_{kl}\rangle - \langle P_{ij}\rangle\langle P_{kl}\rangle$. The reference bond is black, positive (negative) correlations are shown with blue (red dashed) lines. The width of the lines is proportional to the correlation function. The periodic (Wigner-Seitz) cell is shaded in grey. Left panel: Results for the SU(3) Heisenberg model for a $N_s = 21$ kagome sample. Right panel: Results for the SU(4) Heisenberg model on the checkerboard lattice for a $N_s = 20$ sample.

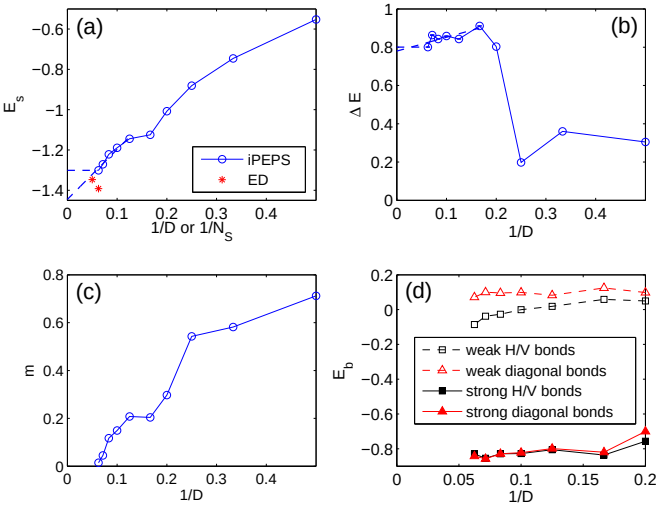

FIG. 5: (Color online) iPEPS simulation results for the SU(4) Heisenberg model on the checkerboard lattice as a function of inverse bond dimension. (a) Energy per site, E_s, compared with the results from ED (plotted as a function of $1/N_s$). (b) Different bond energies in the quadrumerized state. The strong horizontal and vertical bonds (H/V) have the same energy as the strong diagonal bonds for large D. (c) The difference in bond energies ΔE is finite which shows that the state breaks lattice symmetries [cf. Fig. 1(b)]. (d) The local moment decreases rapidly with D and vanishes for large D.

IV. THE SU(4) MODEL ON THE CHECKERBOARD LATTICE

The SU(4) model on the checkerboard lattice is described by the Hamiltonian (1) with the fundamental representation of SU(4) at each lattice site. Thus the local dimension of a lattice site is four.

Figure 5(a) shows the iPEPS energies as a function of inverse bond dimension. We find that even for the largest values of D used the energy still decreases considerably upon further increasing D. In the infinite D limit we expect the energy to lie in the range $-1.45 < E_s < -1.30$. The ED result for finite systems $E_s^{N_s=16} = -1.392$, and $E_s^{N_s=20} = -1.347$ lie within this range.

The difference in bond energies ΔE, shown in Fig. 5(b), becomes large for $D \geq 5$. Not all the weak bonds have exactly the same energy, see Fig. 5(d). So we took averaged energies of the weak and strong bonds to compute ΔE. The distribution of the individual bond energies on the lattice can be seen in Fig. 1(b), clearly showing that quadrumers are formed. With increasing bond dimension ΔE slightly decreases but the data still suggest a rather large value in the range $\Delta E \approx 0.77 - 0.80$ in the infinite D limit.

Figure 5(c) shows that the ordered moment vanishes in the large D limit, compatible with a quadrumerized state which does not break SU(4) symmetry.

Finally, ED results for the connected bond energy correlations are shown in the right panel of Fig. 4 for a $N_s = 20$ sample. They further highlight the strong quadrumerization instability of the checkerboard lattice SU(4) Heisenberg model.

V. DISCUSSION

The iPEPS and exact diagonalization results reported in this paper give clear evidence in favor of the stabilization of simplex solids for SU(3) on kagome and for SU(4) on the checkerboard lattice. The underlying mechanism is the formation of SU(N) singlets on the simplices of the lattice, which is possible whenever N is equal to the number of sites of the simplices. Based on these results we also expect a two-fold degenerate simplex solid ground state for the SU(4) model on the pyrochlore lattice (as suggested by previous work[15,16,18]) as well as the SU(3) model on the Garnet lattice or variants thereof.[15,40]

In principle, it is sufficient that the number of sites be a multiple of N for this scenario to be realized. Interestingly, the SU(2) Heisenberg model on the checkerboard lattice fulfills this condition, and its ground state is also spontaneaously quadrumerized.[41,42] However, the strong bonds form plaquettes on the *empty* squares in that case, and the mechanism is different: the diagonal bonds are instrumental in frustrating the inter-plaquette coupling.

Another interesting conclusion can be drawn regarding flavor-wave theory. In models investigated so far, flavor-wave theory (FWT) has always revealed some aspect of the ground state: it led to the correct ground state for the SU(3) model on the square[43] and the triangular[44] lattices, and it gave interesting insight for the SU(4) model on the square lattice.[29] In the case of SU(3) on kagome reported in this paper, it fails completely: the ground state is predicted to be an ordered state with a $\sqrt{3} \times \sqrt{3}$ unit cell and no trimerization (all bond energies remain equal). In fact, it is simply impossible to describe a trimerized state with FWT since this would required to build an unfrustrated, two-color configuration on a triangle. It is nevertheless amusing to notice that the ground state degeneracy is already lifted at the harmonic level, by contrast to the SU(2) case, and that the $\sqrt{3} \times \sqrt{3}$ state (energy per site of

$-2+2/\sqrt{3} \simeq -0.845$) is favored over the $\vec{q} = \vec{0}$ state (energy per site of $-2+4/\pi \simeq -0.727$), as for the SU(2) case beyond linear spin-wave theory.[45–47] We note that these energies are not variational and thus cannot be compared with the iPEPS energies.

Acknowledgments

The ED simulations have been performed on machines of the platform "Scientific computing" at the University of Innsbruck - supported by the BMWF, and the iPEPS simulations on the Brutus cluster at ETH Zurich. We thank the support of the Swiss National Science Foundation, MaNEP, and the Hungarian OTKA Grant No. K73455.

[1] I. Affleck and J. B. Marston, Phys. Rev. B **37**, 3774 (1988).
[2] J. B. Marston and I. Affleck, Phys. Rev. B **39**, 11538 (1989).
[3] N. Read and S. Sachdev, Phys. Rev. Lett. **62**, 1694 (1989).
[4] N. Read and S. Sachdev, Phys. Rev. B **42**, 4568 (1990).
[5] K. Harada, N. Kawashima, and M. Troyer, Phys. Rev. Lett. **90**, 117203 (2003).
[6] N. Kawashima and Y. Tanabe, Phys. Rev. Lett. **98**, 057202 (2007).
[7] K. S. D. Beach, F. Alet, M. Mambrini, and S. Capponi, Phys. Rev. B **80**, 184401 (2009).
[8] M. Hermele, V. Gurarie, and A. M. Rey, Phys. Rev. Lett. **103**, 135301 (2009).
[9] M. Hermele and V. Gurarie, Phys. Rev. B **84**, 174441 (2011).
[10] C. Wu, J.-P. Hu, and S.-C. Zhang, Phys. Rev. Lett. **91**, 186402 (2003).
[11] C. Honerkamp and W. Hofstetter, Phys. Rev. Lett. **92**, 170403 (2004).
[12] M. A. Cazalilla, A. F. Ho, and M. Ueda, New Journal of Physics **11**, 103033 (2009).
[13] A. V. Gorshkov, M. Hermele, V. Gurarie, C. Xu, P. S. Julienne, J. Ye, P. Zoller, E. Demler, M. D. Lukin, and A. M. Rey, Nat Phys **6**, 289 (2010).
[14] T. A. Tóth, A. M. Läuchli, F. Mila, and K. Penc, Phys. Rev. Lett. **105**, 265301 (2010).
[15] C. L. Henley, Can. J. of Phys. **79**, 1307 (2001).
[16] M. Indergand, A. Läuchli, S. Capponi, and M. Sigrist, Phys. Rev. B **74**, 064429 (2006).
[17] M. Indergand, C. Honerkamp, A. Läuchli, D. Poilblanc, and M. Sigrist, Phys. Rev. B **75**, 045105 (2007).
[18] D. P. Arovas, Phys. Rev. B **77**, 104404 (2008).
[19] I. Affleck, T. Kennedy, E. H. Lieb, and H. Tasaki, Physical Review Letters **59**, 799 (1987).
[20] G. Sierra and M. A. Martin-Delgado, Preprint (1998), arXiv:cond-mat/9811170 .
[21] T. Nishino and K. Okunishi, Journal of the Physical Society of Japan **67**, 3066 (1998).
[22] F. Verstraete and J. I. Cirac, Preprint (2004), arXiv:cond-mat/0407066 .
[23] Y. Nishio, N. Maeshima, A. Gendiar, and T. Nishino, Preprint (2004), arXiv:cond-mat/0401115 .
[24] V. Murg, F. Verstraete, and J. I. Cirac, Phys. Rev. A **75**, 033605 (2007).
[25] S. R. White, Phys. Rev. Lett. **69**, 2863 (1992).
[26] J. Jordan, R. Orús, G. Vidal, F. Verstraete, and J. I. Cirac, Phys. Rev. Lett. **101**, 250602 (2008).
[27] P. Corboz, R. Orus, B. Bauer, and G. Vidal, Physical Review B **81**, 165104 (2010).
[28] P. Corboz, S. White, G. Vidal, and M. Troyer, Phys. Rev. B **84**, 041108 (2011).
[29] P. Corboz, A. M. Läuchli, K. Penc, M. Troyer, and F. Mila, Phys. Rev. Lett. **107**, 215301 (2011).
[30] B. Bauer, P. Corboz, A. M. Läuchli, L. Messio, K. Penc, M. Troyer, and F. Mila, Phys. Rev. B **85**, 125116 (2012).
[31] G. Vidal, Phys. Rev. Lett. **91**, 147902 (2003).
[32] R. Orús and G. Vidal, Phys. Rev. B **78**, 155117 (2008).
[33] H. Jiang, Z. Weng, and T. Xiang, Phys. Rev. Lett. **101**, 090603 (2008).
[34] T. Nishino and K. Okunishi, Journal of the Physical Society of Japan **65**, 891 (1996).
[35] R. Orús and G. Vidal, Phys. Rev. B **80**, 094403 (2009).
[36] S. Singh, R. N. C. Pfeifer, and G. Vidal, Phys. Rev. B **83**, 115125 (2011).
[37] B. Bauer, P. Corboz, R. Orús, and M. Troyer, Phys. Rev. B **83**, 125106 (2011).
[38] P. Corboz, J. Jordan, and G. Vidal, Phys. Rev. B **82**, 245119 (2010).
[39] A. M. Läuchli, J. Sudan, and E. S. Sørensen, Phys. Rev. B **83**, 212401 (2011).
[40] E. J. Bergholtz, A. M. Läuchli, and R. Moessner, Phys. Rev. Lett. **105**, 237202 (2010).
[41] J.-B. Fouet, M. Mambrini, P. Sindzingre, and C. Lhuillier, Phys. Rev. B **67**, 054411 (2003).
[42] B. Canals, Phys. Rev. B **65**, 184408 (2002).
[43] T. A. Tóth, A. M. Läuchli, F. Mila, and K. Penc, Phys. Rev. Lett. **105**, 265301 (2010).
[44] A. Läuchli, F. Mila, and K. Penc, Phys. Rev. Lett. **97**, 087205 (2006).
[45] A. Chubukov, Phys. Rev. Lett. **69**, 832 (1992).
[46] S. Sachdev, Phys. Rev. B **45**, 12377 (1992).
[47] C. Henley and E. Chan, J. Magn. Magn. Mater. **140-144**, 1693 (1995).
[48] A N-site simplex is a cluster of N sites in which each site is connected to all the other sites.
[49] We have kept the terminology simplex solid introduced by Arovas in Ref. 18. However, since a lattice symmetry is broken in the ground state, leading to a two-fold degeneracy, it is better seen as a generalization of a valence bond crystal in the terminology of SU(2) valence bond states. In Ref. 9 these states were called *valence cluster states*.

arXiv:1204.6682v2 [cond-mat.str-el] 2 Aug 2012

Supplementary material

Philippe Corboz,[1] Karlo Penc,[2,3] Frédéric Mila,[4] and Andreas M. Läuchli[5,6]

[1]*Theoretische Physik, ETH Zürich, CH-8093 Zürich, Switzerland*
[2]*Institute for Solid State Physics and Optics, Wigner Research Centre for Physics, Hungarian Academy of Sciences, H-1525 Budapest, P.O.B. 49, Hungary*
[3]*Department of Physics, Budapest University of Technology and Economics and Condensed Matter Research Group of the Hungarian Academy of Sciences, 1111 Budapest, Hungary*
[4]*Institut de théorie des phénomènes physiques, École Polytechnique Fédérale de Lausanne, CH-1015 Lausanne, Switzerland*
[5]*Institut für Theoretische Physik, Universität Innsbruck, A-6020 Innsbruck, Austria*
[6]*Max-Planck-Institut für Physik komplexer Systeme, Nöthnitzer Straße 38, D-01187 Dresden, Germany*

(Dated: March 3, 2013)

I. DETAILS ON THE SETUP 2 TO SIMULATE THE KAGOME MODEL

Here we explain how to map a nearest-neighbor Hamiltonian on the kagome lattice $\hat{h}$ onto a nearest-neighbor Hamiltonian on the square lattice $\hat{H}$, where three physical sites A, B, C on the kagome lattice are blocked into one block site of the square lattice, as shown in Fig. 2(b) in the main text. The Hilbert space of a block site $\mathcal{H}_{BS}$ is given by

$$\mathcal{H}_{BS} = \mathcal{H}_A \otimes \mathcal{H}_B \otimes \mathcal{H}_C, \tag{1}$$

where $\mathcal{H}_A$, $\mathcal{H}_B$, $\mathcal{H}_C$ are the local Hilbert spaces of the three physical sites A, B, C, respectively. Thus, for the SU(3) Heisenberg model with local physical dimension 3 the local dimension of a block site is $3^3 = 27$.

The original Hamiltonian defined on the kagome lattice is given by

$$\hat{h} = \sum_{\langle u,v\rangle} \hat{h}_{u,v}, \tag{2}$$

where the sum $\langle u, v\rangle$ goes over nearest-neighbor sites on the kagome lattice. The Hamiltonian $\hat{H}$ defined on the lattice formed by the block sites reads

$$\hat{H} = \sum_i \hat{H}^s_i + \sum_{\langle i,j\rangle_x} \hat{H}^x_{i,j} + \sum_{\langle i,j\rangle_y} \hat{H}^y_{i,j} \tag{3}$$

where the sum i goes over all block sites in the square lattice, and $\langle i, j\rangle_x$ and $\langle i, j\rangle_y$ are sums over nearest-neighbor pairs in x-direction and y-direction, respectively. Each site term $\hat{H}^s_i$ contains two terms of the original Hamiltonian (2):

$$\hat{H}^s_i = \hat{h}_{i_A,i_B} + \hat{h}_{i_A,i_C}, \tag{4}$$

where h_{i_A,i_B} ($\hat{h}_{i_A,i_C}$) is the Hamiltonian term connecting the physical sites A and B (A and C) on block site i. These two terms correspond to the horizontal and vertical blue lines within a block site in Fig. 2(b). In x-direction the block Hamiltonian is given by the sum of two contributions,

$$\hat{H}^x_{i,j} = \hat{h}_{i_B,j_A} + \hat{h}_{i_B,j_C}, \tag{5}$$

where i_B is the B-site on block site i, and j_A is the A-site of the neighboring block site j. The first (second) term corresponds to the horizontal (diagonal) blue line in Fig. 2(b) which connect two neighboring block sites in x-direction. Similarly, the block Hamiltonian term in y-direction reads

$$\hat{H}^y_{i,j} = \hat{h}_{i_C,j_A} + \hat{h}_{i_C,j_B} \tag{6}$$

where the first (second) term corresponds to the vertical (diagonal) blue line in Fig. 2(b) which connect two neighboring block sites in y-direction.

Thus, we find that the Hamiltonian (3) defined on the block site lattice is a nearest-neighbor Hamiltonian on the square lattice, which can be simulated with the standard iPEPS method for the square lattice.

We point out that the correlations within a block site are taken into account in an exact way, whereas the correlations between physical sites on neighboring block sites depend on the bond dimension D. Thus, by performing the blocking we favor correlations between the three physical sites in a block site, which can bias the result for small bond dimensions. However, as we note in the paper, we do not block the three sites which eventually form a singlet (if we would do this we would bias the state to a singlet state from the start, i.e. a trivial $D = 1$ PEPS could already represent a trimerized state). This bias becomes irrelevant for large bond dimensions, because for large D the physical sites on neighboring block sites can also become strongly correlated. Indeed, as we show in the paper, at large bond dimensions the results become equivalent with the ones obtained with the simulation setup I, where we did not use this blocking.